Chapter 3 Simulated Results and Discussion

3-1 Equal frequency surface and effective refraction index

The propagation of EM waves through a photonic crystal, which is a highly inhomogeneous medium in its nature. This makes it difficult to describe the propagation behavior in a simple accurate way. However, recently a lot of theoretical and experimental practices [9,11] have shown that the overall behavior of the wave propagation within a photonic crystal can be well described by a model based on the equal frequency surface (EFS) configuration of the photonic crystal and the related group velocity, which is parallel to the EFS normal direction. An example for the EFS contour in $\vec{k}$ space (contour in the 2D system) [9], shown in Fig. 3-1, basically consists of the allowed propagation modes within the crystal for several certain frequencies. It is the important physics picture which can help us to qualitatively explain the propagation properties in photonic crystals.

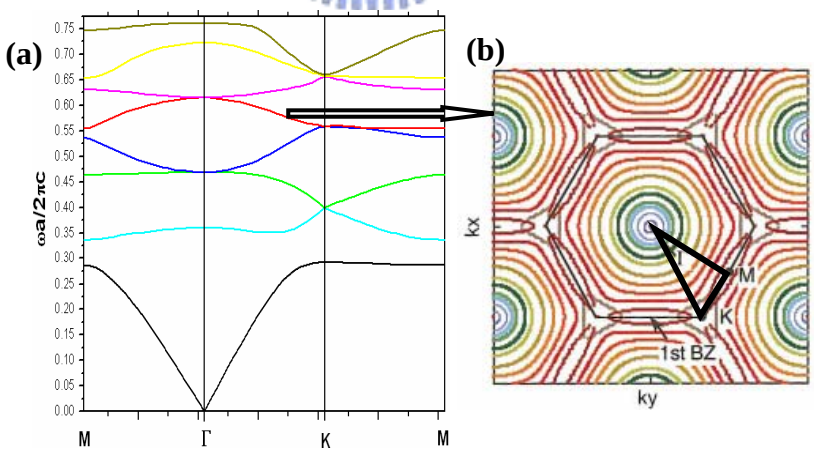

Fig.3-1 (a) A band structure of photonic crystal. (b) A equal frequency surface (EFS) of the 5th band. The center region of EFS is the 1st Brillouin zone.

In photonic crystal, the propagation direction of light is highly related to the EFS. We

can show the reciprocal lattice space to describe the phenomenon. Note that the direction in reciprocal space exactly corresponds to that in real space because of the symmetry.

Firstly, we show a very simple example of EFS analysis which is calculated by plane wave expansion (PWE) method, as Fig. 3-2. It describes a light incident problem from air to a photonic crystal. This shows that an EFS expression of conventional refraction phenomenon at the interface for two different media, and this plot is a graphical representation of Snell's law in *k* space. The inner and outer circles are the EFS of the photonic band of the air and photonic crystal, namely, $\omega_{air} = ck_i / n_i$ and $\omega_{PC} = ck_f / n_{PC}$. Fig. 3-2(b) and (c) are representative for the first band and second band EFS of air and photonic crystal with a certain frequency. In Fig. 3-2(a), a photonic band structure with the fundamental and second bands, the group velocities ($\vec{v}_g$) for the first and second photonic band are positive and negative respectively, which means that the frequency increases outward for the case of first band while it increases inward for the case of second band. In other words, the direction of group velocity is the direction of gradient of the frequency ($\nabla_k \omega$). So the direction of group velocity is outward from the circular EFS in Fig. 3-2(b) and is inward from the circular EFS in Fig. 3-2(c), in addition which are normal to the EFS. Meanwhile, the direction of group velocity vector is the direction of the energy flow for an infinite PC system, so the group velocity vectors in the figures represent the directions of propagation for the EM signal in the dielectric.

The *k* vector in the photonic crystal (i.e. $\vec{k}_f$) is determined by the continuity of tangential components of the *k* vector (i.e. $k_{||}$) across the interface (more precisely, the phase continuity).

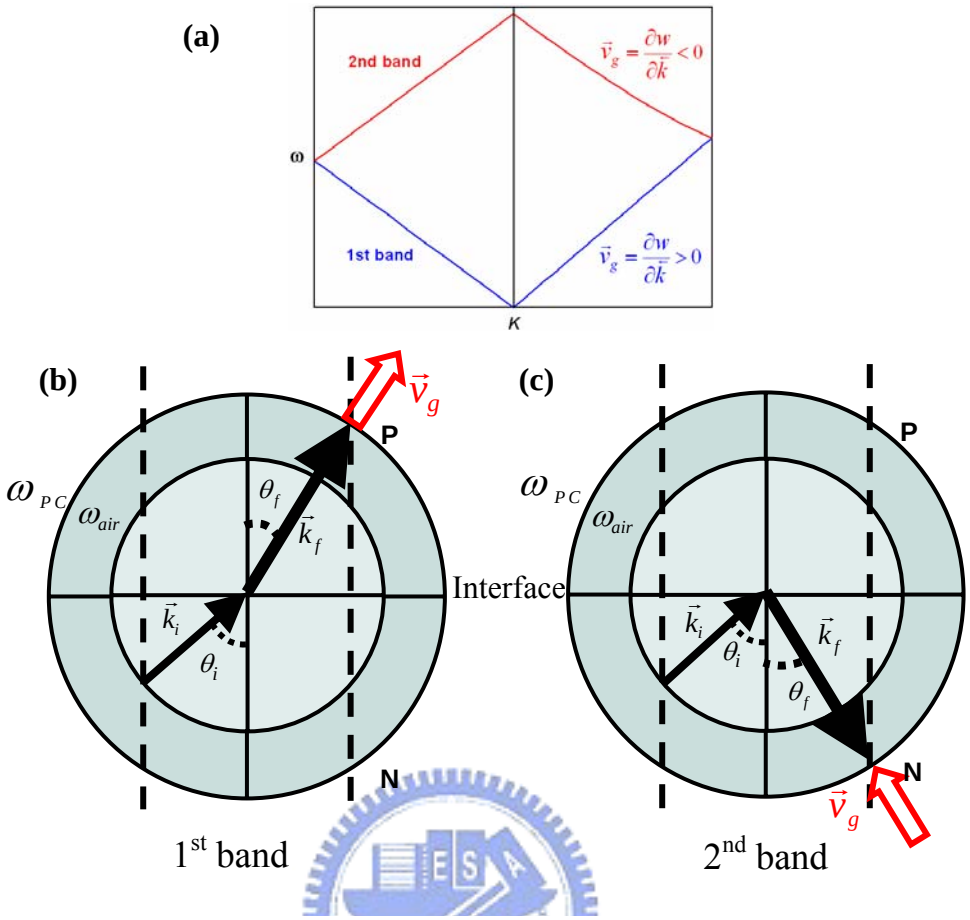

Fig.3-2 (a) A photonic band structure with the 1st and 2nd bands. Schematics of wave-vector diagrams to show the wave propagation from air to a photonic crystal with frequency in (b) 1st band and (c) 2nd band. The inner and outer circle is the EFS of the photonic band of the air and photonic crystal with a certain frequency. The dashed line represents the conservation of the parallel component of the wave vector.

The $k_{\|}$ conservation condition given by the dashed vertical line in the figures determines the allowed refracted wave vector $\vec{k}_f$. When an incident wave vector $\vec{k}_i$ got to the interface from the air with an oblique angle, there are two choices for $\vec{k}_f$ (to point either toward P or toward N). We know that the second band of reciprocal lattice space is folded into the first Brillouin zone taking into account the identity of the wave numbers (i.e. $\vec{k}_f$) which differ from each other by a multiple of G, a reciprocal lattice vector. Therefore taking

this into consideration, the correct choice for $\vec{k}_f$ is to point toward *P* for the case of Fig. 3-2(a) and toward *N* for the case of Fig. 3-2(b). For every choices $\vec{k}_f$, the $\vec{v}_g$ will be normal to the EFS at that point and point toward increasing values of frequency.

In a photonic crystal, owing to the shape of EFS (i.e. the inner part of Fig. 3-1 (b)) is almost circular (circular-like) for the higher frequencies, which means that the wave propagation is isotropic-like at these frequencies. For the isotropic frequency range, the effective refraction index concept can be used for description of light propagation, and light refraction is simply described by the Snell's law in (3.1). [9] (The effect of the photonic crystal arose from a modification of the mixing ratio of index values, similar to the way in which the effective refraction index of a conventional slab wave guide is derived. [21])

$$\sin\theta_1 / \sin\theta_2 = n_2 / n_1 \tag{3.1}$$

This effective refraction index is the phase index of refraction since it is defined from the phase velocity:

$$\left|n_{eff}\right| \cong \left|n_p\right| = {c\left|\vec{k}_f\right|}\Big/{\omega} = {\left|\vec{k}_f\right|}\Big/{\left|\vec{k}_0\right|} \tag{3.2}$$

Where k_f and k_0 are the wave vector in the photonic crystal and in vacuum, respectively. The sign of n_p is determined from the behavior of EFS. If the EFS move outward with increasing frequency, i.e. $\vec{v}_g \bullet \vec{k}_f > 0$, then n_p is positive; if they move inward, i.e. $\vec{v}_g \bullet \vec{k}_f < 0$, then n_p is negative. Because the group velocity coincides with the energy velocity, the sign of $\vec{v}_g \bullet \vec{k}_f$ is equivalent to the sign of $\vec{S} \bullet \vec{k}_f$. So, in order to be in accordance with the LH literature, the sign of n_p will be the sign of $\vec{v}_g \bullet \vec{k}_f$.

We notice that in some frequencies of photonic crystal, the EFS can have different

shapes for various angles. Therefore $\vec{k}_f$ and $\vec{v}_g$ are not parallel to each other due to the shapes of EFS are not circular-like. These phenomena as we will see at the outer part of Fig. 3-1 (b), in other words, the effective refraction index concept will exhibit apparent errors in this case.

3-2 Refractive phenomena in photonic crystal prisms

3-2.1 Photonic band structures and symmetry of eigenmode patterns

In order to understand the left-handed behavior in photonic crystals is possible and distinguish the differences between the positive and negative refraction phenomena, we consider the problem an incoming electromagnetic wave incidents on a photonic crystal. The simulative frame is a two-dimensional photonic crystal which is a periodic triangular array of air rods in dielectric material with dielectric constant 10.5. The radius of the air rods is r=0.35a, where a is the lattice constant. We know that the most interested two-dimensional photonic crystal structure is triangular lattice of air rods, which possesses a photonic band gap for transverse electric mode (i.e. TE mode). However, the formation of well-defined effective index states prefers transverse magnetic mode (i.e. TM mode) [22], so we consider it only here.

In Fig. 3-3, the photonic band structure (PBS) of the system which is calculated by plane wave expansion (PWE) method. There is no band gap for TM mode consists of fundamental band and second band in our photonic crystal structure. The quantity $\tilde{\omega}$ is the frequency normalized as $\omega a/2\pi c$, where c is the velocity of light. We knew yet what the photonic band structures represent the existence of photon density of states, that is, the transmission spectra

in photonic crystals can be investigated by the distribution of eigenmodes. Although the kind of comparison is correct concernment, it neglects the effect of the coupling strength between the incident/transmitted wave and the internal electromagnetic field at the surface of the photonic crystal structures, the energy transfer to Bragg waves, and the interference between the front and the rear surface.

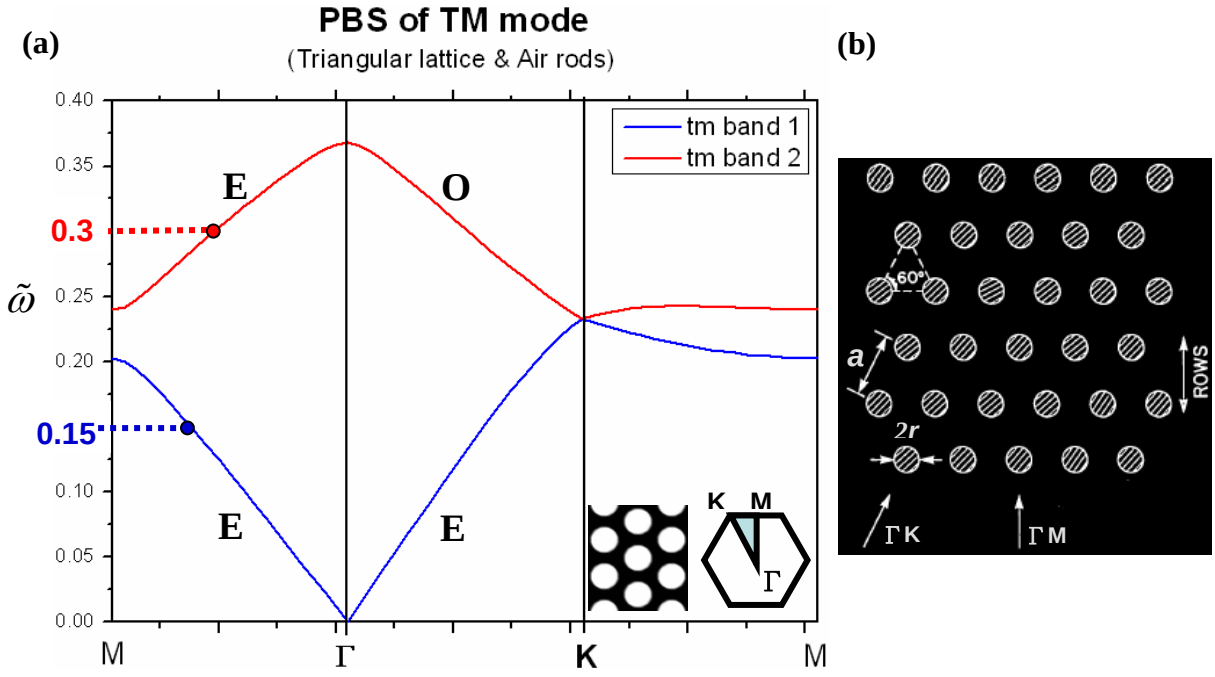

Fig.3-3 (a) TM-mode photonic band structure of 2-D photonic crystal with a triangular lattice of air rods. (b) Triangular-lattice configuration, showing the lattice *a*, air-rod radius *r*, and principal symmetry directions (ΓM and ΓK).

In fact, the eigenmodes of photonic crystal are classified to coupled modes and uncoupled modes, and the coupling strength is dependent of them. Where the coupled mode and uncoupled mode stands for the symmetry and antisymmetry of eigenmode patterns, individually. [22,23] The existence of the uncoupled modes, or the eigenmodes of the lattice that cannot be excited by an external plane wave, was first pointed out by Robertson *et al.* [24] They compared the dispersion relation of 2D lattices observed by their coherent microwave

transient spectroscopy technique with that by the band calculation, and they found that the antisymmetric modes under the mirror reflection that belongs to the intrinsic symmetry operations of the point group of the lattice were not observed in their experiments. They concluded that the incident plane wave does not excite these antisymmetric modes because the former is symmetric under the same mirror reflection, and hence the effective coupling between them is absent.

This is an important statement for our simulations of the following sections due to the frequencies (i.e. eigenmodes) we chose need to be allowed exciting and propagating in the photonic crystals. We now explain the dependence of symmetry on excitation of eigenmodes by a reflective method of mirror plane which is proposed by Robertson *et al.*, as the samples shown in Fig.3-4. [25] The mirror planes stand for propagation along the ΓM directions of the square lattice (These are special directions in the Brillouin zone) are indicated by dashed lines; physically, the field patterns associated with the various modes must be either even or odd on reflection through the mirror planes. Observably, the mode patterns are even for the case (a) and odd for the case (b).

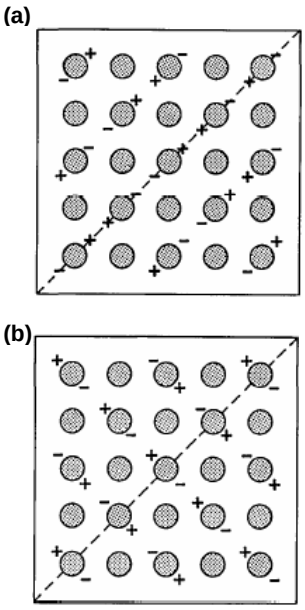

Fig.3-4 Symmetry of eigenmode patterns of the square lattice for propagation along the ΓM directions. The states depicted lie at the k=(1/2,1/2) point of the Brillouin zone. +(−) indicate regions in which the field is oriented into (out of) the page. The modes are (a) even and (b) odd with respect to the mirror plane, shown as the dashed lines.

Here we also calculate the eigenmodes of TM for our simulative structure which is triangular lattice with air rods in dielectric by using the plane-wave expansion method, in Fig.3-5. This figure shows a plot of the calculated field patterns for the 1st band and the 2nd band in ΓM direction, cases (a) and (b), and in ΓK direction, cases (c) and (d). All of these modes are even (i.e. symmetric) under reflection mirrors except for case (d), which is odd (i.e. antisymmetric), where the blue (red) indicates to negative (positive) electric fields. So we can predict that the excitation of the second band in ΓK direction by an incoming plane wave which is symmetric mode is forbidden, and we will study the problems of refraction that focus on the certain frequencies of 1st and 2nd band for ΓM direction later.

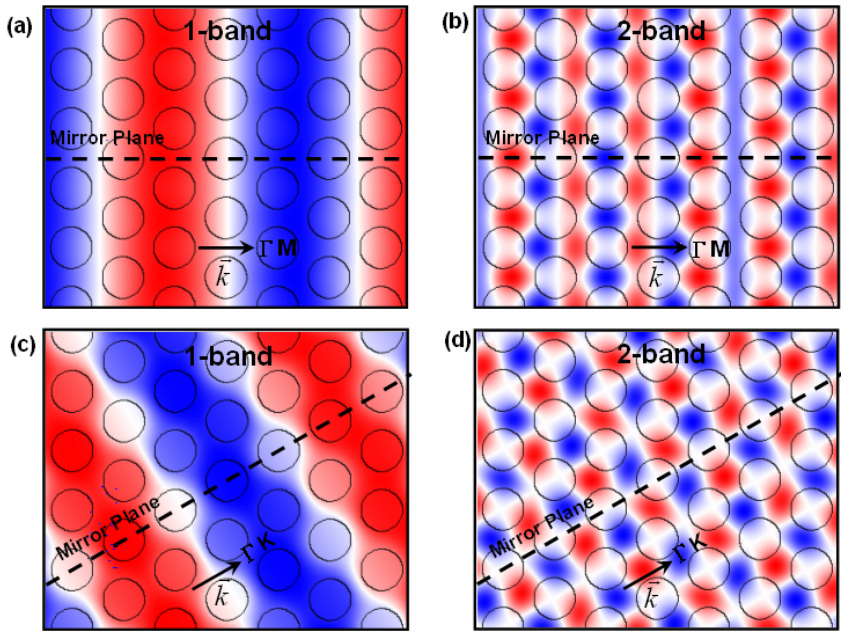

Fig.3-5 Schematic of the symmetry of eigenmode patterns of the triangular lattice for propagation along the ΓM directions, as (a) 1st band and (b) 2nd band, and for propagation along the ΓK direction, as (c) 1st band and (d) 2nd band. The blue (red) indicates to negative (positive) electric fields. The mode patterns with respect to the mirror plane, shown as the dashed lines are even for (a), (b), and (c), but odd for (d).

3-2.2 Predictions of propagation vectors in real space

M. Notomi made an argument that the fundamental band and second band are individually the positive-index state and the negative-index state. Regarding the characteristics, there is an interesting analogy with the electronic band in semiconductors, as shown in Fig. 3-6. [9] In a semiconductor, a negative effective mass (the hole band) appears below the energy gap, and a positive effective mass (the electron band) appears above the gap, which is quite similar to the manifestation of effective index in photonic crystals. This analogy makes sense if we note that the sign of effective mass in semiconductors and the sign of effective index in photonic crystals are both derived from the band curvature.

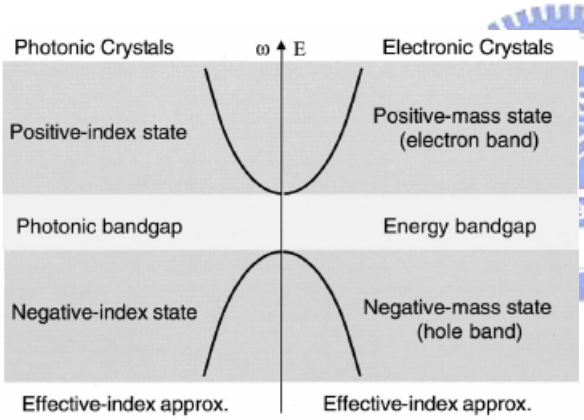

Fig.3-6 Analogy between effective mass approximation for Bloch electron bands and effective index approximation for Bloch photon band.

We can discover some properties from the three-dimensional photonic band structure (3-D PBS) as shown in Fig. 3-7(a) and (b). The fundamental band (1st band) near the 1st band edge sees as conic which top is downward, and all of the group velocities on the surface are positive. The second band (2nd band) near the 1st band edge sees as conic which top is upward, and the all group velocities on the surface are negative. For the low frequency (or long wavelength) part of the 1st band, it is similar to a conventional isotropic dielectric material, i.e. the wave propagating in the PC does not feel the modulation due to the periodic structure. Nevertheless, for the 2nd band, the photonic bands are not. We might expect that photonic

band is strongly modulated.

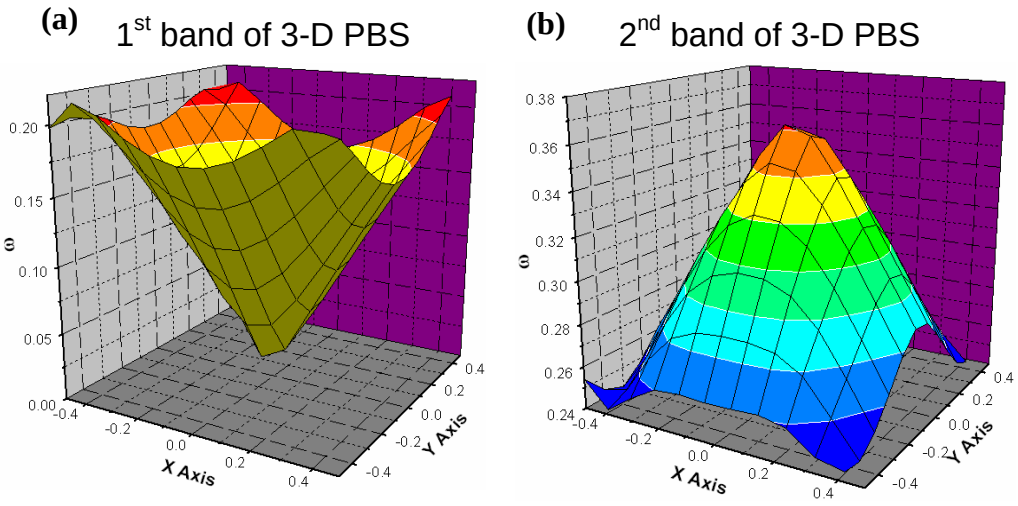

Fig.3-7 The 3-D representation of the photonic band structures for (b) 1st band and (c) 2nd band.

Fig. 3-8(a) and (b) show the equal frequency surface (EFS) plot for the fundamental band, between the normalized frequencies 0 and 0.24, and second band, between the normalized frequencies 0.22 and 0.38 respectively. The part of dark-blue shade has a higher frequency and the dash line is the first Brillouin zone. In Fig. 3-8(a), the shape of 1st band EFS is almost circular owing to weakly modulated of periodicity, where the wave vector ***k*** and the group velocity $\vec{v}_g$ are parallel each other [but are anti-parallel in the 2nd band as Fig. 3-8(b).] Meanwhile, the direction of group velocity $\vec{v}_g = \nabla_k \omega$ is normal to EFS and toward frequency increasing way. Furthermore, we can see that higher frequencies region of 2nd band is circular-like which has isotropic feature. For these frequency ranges, the concept of effective refraction index can be used for describing refractive phenomena by the Snell's law. We chose the simulative frequencies 0.15 and 0.3 for the 1st and 2nd band consequent on isotropic property in the following section.

First, we might study the schematics of propagation vectors in real space, as shown in

Fig. 3-9. This way can show that theoretically predicted refracted behavior at the interface

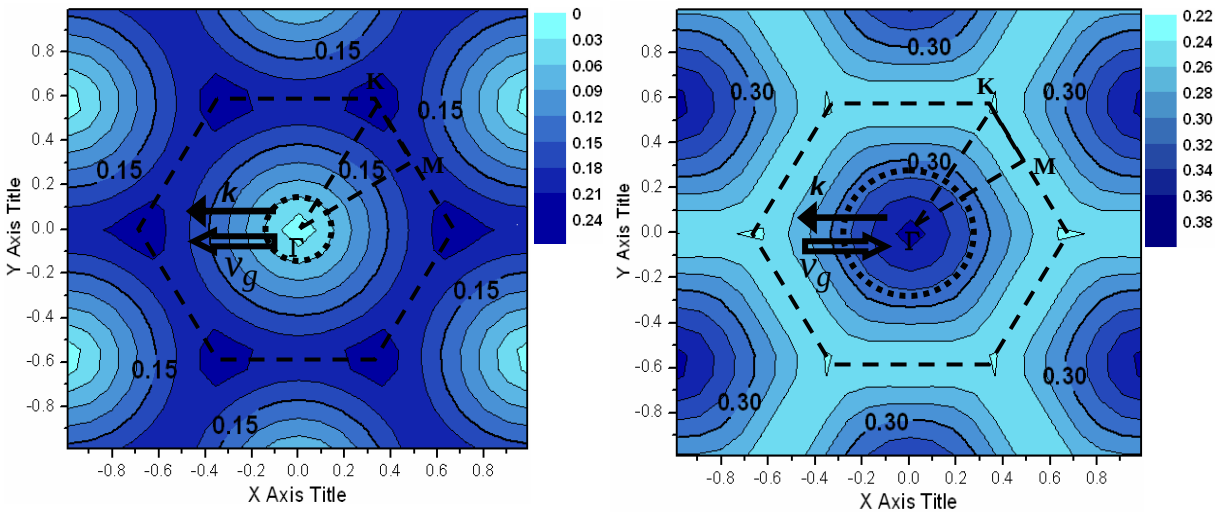

Fig.3-8 Schematic pictures of the equal frequency surface (EFS) for the (a) 1st band, normalized frequencies 0—0.24, and (b) 2nd band, normalized frequencies 0.22—0.38. The part of dark-blue shade has a higher frequency and the dash line is first Brillouin zone. Where the thick lines are for the simulative frequencies 0.15 and 0.3 that we chose, moreover, the dot lines are for these frequencies in the air.

between photonic crystal and air by using the EFS concept, moreover, it will profit to compare the properties of infinite system with the result in the FDTD (finite-difference time-domain) simulation. Where the circle of solid line is frequency contour 0.15 in photonic crystal for case (a) and 0.3 for case (b) respectively. Besides, the circle of dot line is frequency contour in air for these two frequencies. The $k_{\parallel}$ conservation condition given by the dashed vertical line in the figures determines the allowed refracted wave vector $\vec{k}_f$. An incident wave vector $\vec{k}_i$ hits normally the 1st interface along direction ΓM of the first Brillouin zone.

In Fig. 3-9(a), the refractive wave vector $\vec{k}_f$ is parallel with group velocity $\vec{v}_g$, i.e.

$\vec{v}_g \bullet \vec{k}_f > 0$, due to the EFS move outwards from the center with increasing frequency, so there is the right-handed (RH) rule at the 1st and 2nd interfaces. That is the final outgoing electromagnetic wave (i.e. the 2nd refractive wave vector $\vec{k}_{f2}$) will is in the positive hemisphere. However, the $\vec{k}_f$ and $\vec{v}_g$ are anti-parallel each other, i.e. $\vec{v}_g \bullet \vec{k}_f < 0$, due to the EFS move inwards from the center with increasing frequency, then the left-handed (LH) rule will happen, as shown in Fig. 3-9(b). That is $\vec{k}_{f2}$ will is in the negative hemisphere. Observably, the energy flow (i.e. $\vec{v}_g$) propagate forward in photonic crystal owing to the energy flow, i.e. pointing vector $\vec{S}$, always points away from the source. Nevertheless, the $\vec{k}_{f1}$ points forward for the case (a) in and backward for the case (b).

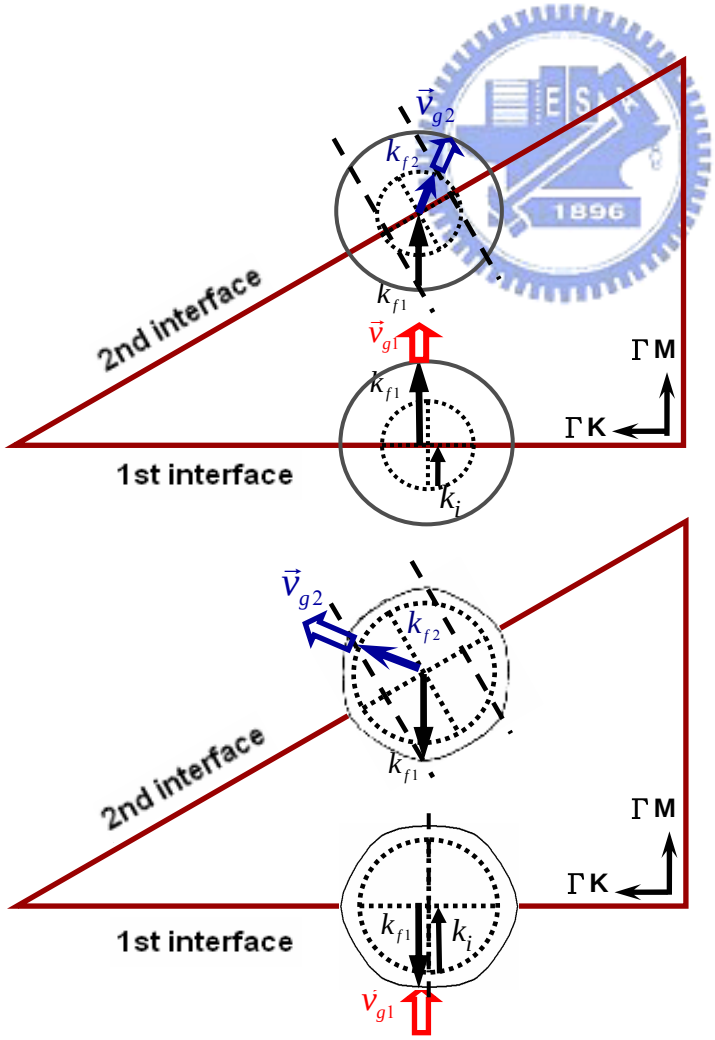

Fig.3-9 Schematic diagram of predicted propagation vectors in real space for (a) positive and (b) negative refraction. The dashed line represents the conservation of the parallel component of the wave vector. The circles of solid line are the frequency contours in photonic crystal and the circles of dot line are frequency contours in air.

3-2.3 Positive refraction, negative refraction, and total internal reflection

Owing to clearly describe the positive and negative refraction phenomena in photonic crystal and compare with the numerical calculation of infinite structure by the plane wave expansion method, we used the finite-difference time-domain (FDTD) method [19] to construct a simulative frame what is an electromagnetic plane wave directed incident normally on a two-dimensional photonic crystal prism (PCP) along ΓM direction from the air, as shown in Fig. 3-10.

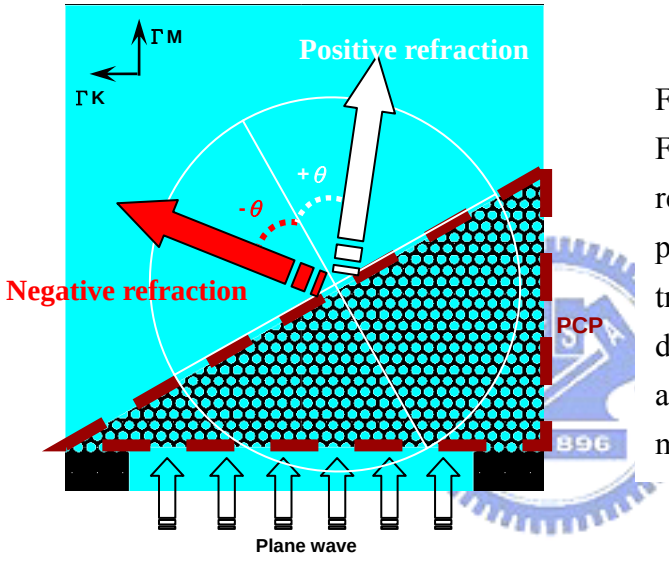

Fig.3-10 Schematic diagram of our FDTD simulative frame. This region for the dash line is a photonic crystal prism (PCP) with triangular lattice air rods in dielectric. The light-color part is air, and the dark-color part is dielectric material (ε=10.5).

The simulations are performed using the FDTD method, and the perfectly matched layers (PML) are used for the absorbing boundaries shown as the dash line in Fig. 3-11. In particular, we illustrate the results of simulation, using a monochromatic plane wave of TM mode, for $\tilde{\omega} = 0.15$ of the 1st band and $\tilde{\omega} = 0.3$ of the 2nd band in the ΓM direction which are allowable excitation, as shown in Fig. 3-3. We got a good consistency in results between the prediction of EFS configuration and the FDTD simulation. For each of these cases, the $k_{\parallel}$ wave vector will be conserved at both of these interfaces, and the final outgoing waves $\vec{k}_{f2}$ propagate into the positive and negative directions for cases (a) and (b) individually.

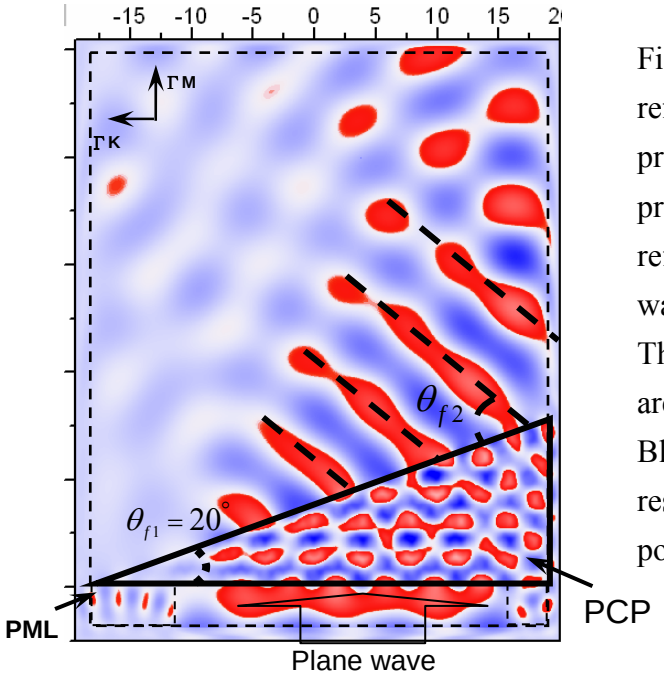

Fig.3-11 FDTD simulations of wave refraction showing the wave fronts propagating across the photonic crystal prism (PCP). Positive and negative refractions happened at the incoming wave frequency (a) 0.15 and (b) 0.3. The perfectly matched layers (PML) are used for the absorbing boundaries. Blue, white, and red correspond, respectively, to negative, zero, and positive E_y.

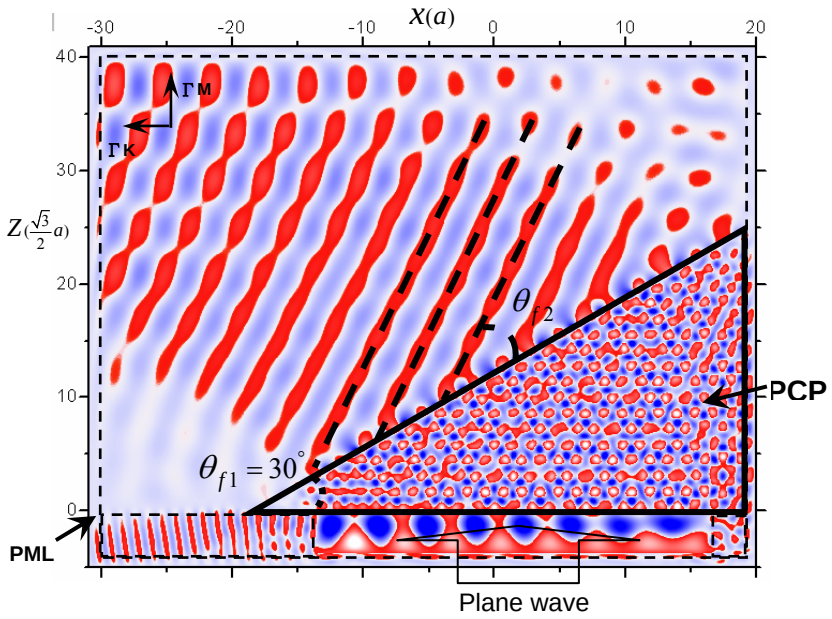

In addition, the wave fronts can be clearly seen at a positive angle $\theta_{f2} = +61^\circ$ and a negative angle $\theta_{f2} = -34^\circ$ with the 2nd interface of refraction. Furthermore, we can using the Snell's law, $n_{eff} \sin\theta_{f1} = n_{air} \sin\theta_{f2}$, to obtain the $n_{eff} \cong 2.56$ with $\theta_{f1} = 20^\circ$ in Fig. 3-11(a) and the $n_{eff} \cong -1.12$ with $\theta_{f1} = 30^\circ$ in Fig. 3-11(b). Where the refractive index of air (n_{air}) is 1. Otherwise, some weakly refraction waves also are seen in the figure. They are the multiple scattering in photonic crystals or edge effect of prism as a result of the finite scale

frame.

The effective refraction index is a function of ω, i.e. $|n_{eff}| = c|\vec{k}_f|/\omega$, and the sign of n_p is determined from the behavior of EFS. Therefore we can calculate it and plot a figure for $n_{eff} - \omega$ relation, as shown in Fig. 3-12. As the effective refraction index is also represented by $|n_{eff}| = |k_f / k_o|$, we use the data in EFS to obtain them for (a) 1st and (b) 2nd band in ΓM direction, where k_f and k_0 are the wave vector along the ΓM direction of the photonic crystal and in air. In other words, the effective refraction index is a fraction of the radius of photonic crystal EFS circle to the radius of air EFS circle at the particular frequency. As the Fig. 3-12 indicates, the effective refraction index is 2.575 for normalized frequency 0.15 of the 1st band in case (a) and is -1.1 for normalized frequency 0.3 of the 2nd band in case (b). Taking these to compare with the measured values in FDTD simulation, we can get a pretty well consistence even if a few errors still existed. Our deduction for the exhibition of errors that the structure of FDTD simulation is finite size and the frequency contours of incoming wave are not really circular (i.e. smooth).

A mentionable details in our simulations, "why didn't we use the same oblique angles $\theta_{f1} = 30^\circ$ of PCP frame for both the ω=0.15 and ω=0.3, as Fig. 3-11 (a) and (b)?", if the effective refraction index for the positive refraction case is calculated, we will notice that total internal reflection happened in this case with a critical incident angle $\theta_c = 23^\circ$. Accordingly, we constructed a frame of the case (a) which oblique angle θ_{f1} is 20° (the condition that electromagnetic wave can transmit across the 2nd interface is $\theta_{f1} < \theta_c = 23^\circ$). In Fig. 3-13, the PCP frame with an oblique angle 23°, the phenomenon of total internal reflection occurs in the 2nd interface. The refractive wave front propagates along the interface can be seen

observably.

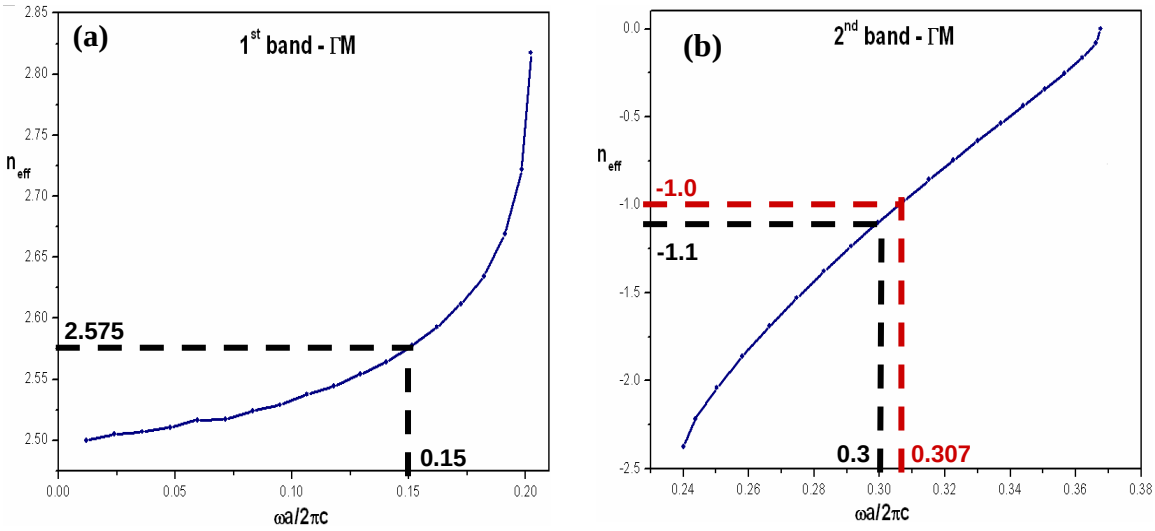

Fig.3-12 Effective refraction index as a function of ω for (a) the 1st band and (b) the 2nd band in ΓM direction of photonic band structure.

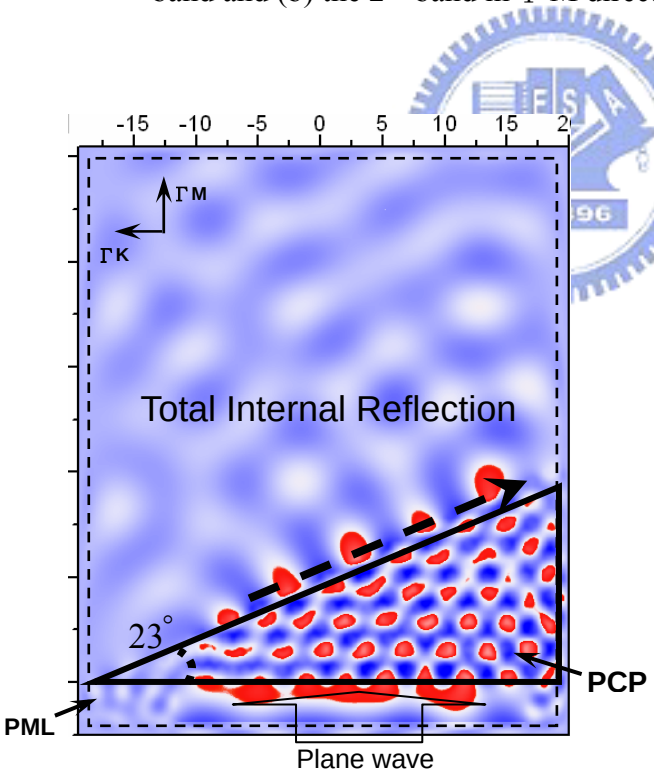

Fig.3-13 FDTD simulations of wave refraction showing the total internal reflection phenomenon. The wave fronts propagating along the 2nd interface between air and photonic crystal prism (PCP). Where the angle of total internal refraction is 23°.

As shown in Fig. 3-5(d), we have already predicted that the eigenmodes of 2nd band along the ΓK direction of our photonic crystal frame are antisymmetric, that is, the existence of the uncoupled modes must exhibit here. We also test the argument presently by FDTD

method. Fig. 3-14 schematically illustrates the uncoupling effect owing to the incident plane wave with normalized frequency 0.3 along the ΓK direction of the Brillouin zone can't permit exciting in this prism, even though the mode lie on the allowed band. For this reason, we can conclude that a problem of refraction in photonic crystals not only needs to study the band structure and the EFS configuration, but also consider the dependence of symmetry on excitation of eigenmodes.

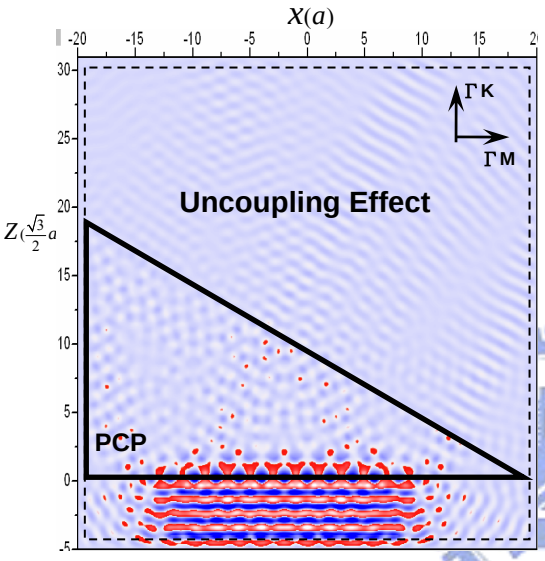

Fig.3-14 FDTD simulation of the uncoupling effect owing to the incident plane wave with normalized frequency 0.3 along the ΓK direction of the Brillouin zone can't permit exciting in the photonic crystal prism.

3-3 Anomalous imaging in photonic crystal slabs with negative refraction

3-3.1 Focusing effect

We know that operation of classical optics: curved surfaces focus light by virtue of the refractive index contrast. Equally their limitations are dictated by wave optics: no lens can focus light onto an area smaller than a square of wavelength. Recently developed artificial media, called the left-hand-materials (LHM), have become of interest because it is the foundation for a variety of novel phenomena [2]. These left-hand-materials exhibit unusual

properties such as negative index of refraction, antiparallel wave vector and Poynting vector ($\langle \mathbf{S} \rangle \cdot \mathbf{k} < 0$), antiparallel phase and group velocities [26]. To develop the negative refraction in the optical regime, one may turn to photonic crystals which essential explanation of these negative refractions should lay in the photonic band structure (PBS) and equal frequency surface (EFS). Furthermore, such a crystal behaves as a material having an effective refractive index, which can be negative, controllable by the PBS [9].

In this section, we would make efforts in this topic what imaging in virtue of focus effect in a two-dimensional photonic crystal slab with negative refraction. Our numerical calculations were performed on a two-dimensional (2D) triangular lattice photonic crystal slab, 8-rows of infinitely air holes, surrounded by dielectric materials with dielectric constant 10.5. The radius of the air rods is r=0.35a, where a is the lattice constant. These material parameters of photonic crystal had been used in section 3-2. The photonic band structure (PBS) is described as Fig. 3-3, the PBS of the TM-polarization, i.e. the electric field polarization paralleled to the air rods, which is calculated by using the plane wave expansion method (PWE). We already realized that the fundamental band and second band are the positive-index state and the negative-index state individually; moreover, we can anticipate that negative refraction phenomena exist in the second band as a result of the outcome in section 3-2.3.

To observe the anomalous focus effect in the photonic crystals with negative refraction, we further simulate wave propagations through the photonic crystal, employing a finite-difference time-domain (FDTD) technique [19]. Our simulative frame is shown in Fig. 3-15. The source starts gradually directed emitting at t=0, a monochromatic TM wave, with Gaussian amplitude which beam width is two times of lattice a. Two sides of the 8-rows photonic crystal slab are the dielectric material with dielectric constant 6.0. We follow the

time and space evolution of the emitted EM waves as the field reaches the steady state. The perfectly matched layers (PML) are used for the absorbing boundaries.

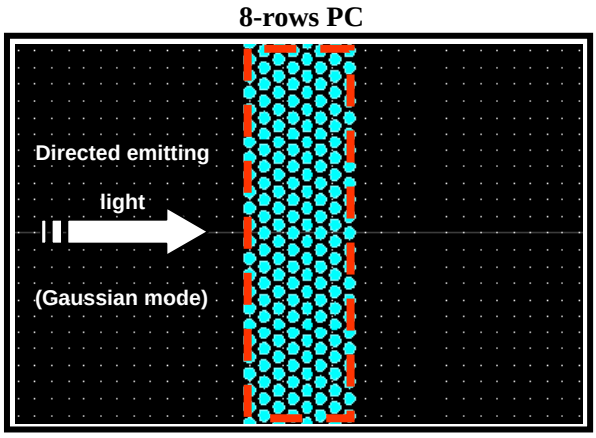

Fig.3-15 Schematic picture of a simulative structure. Where the region of dark color is dielectric materials (ε=6.0), and the center part of figure is a 8-rows photonic crystal slab.

In Fig. 3-16, the emitted wave of normalized frequency ($\tilde{\omega}$) are 0.15 and 0.3 respectively, same as choice of section 3-2.3, several interesting things can be noticed. For the fundamental band at the low frequency ($\tilde{\omega}$=0.15), the wave propagating in the photonic crystal bulk doesn't feel the modulation due to the periodic structure, and the wave beam gradually spread out in Fig. 3-16(a). So the slab is similar to those of a conventional isotropic dielectric material. Besides, for the second band at the high frequency ($\tilde{\omega}$=0.3), we distinctly discover the introduced section of the slab makes the beam focus, owing to an effectively negative refractive index medium bend light to a negative angle with the surface normal, in Fig. 3-16(b). Namely light formerly diverging from the source is set in reverse and converges back to a 1st focal point (1st F. Pt.), and further generates a 2nd focal point (2nd F. Pt.) after the light emerging from the slab. We also represent that longitudinal distribution of the square of electric field along x=0 (i.e. z axis). There are two local maximum values inside the slab and at right side of slab respectively following the source point in Fig. 3-16(d). Nevertheless, there is an exponential decay in Fig. 3-16(c). Hence, we can say that focal points are located at the positions of energy assembling.

Similarly, we can use again the schematic of propagation vectors in real space, as shown in Fig. 3-17. This way can show that theoretically illustrated refracted behavior at the boundaries of photonic crystal slab by using the EFS concept.

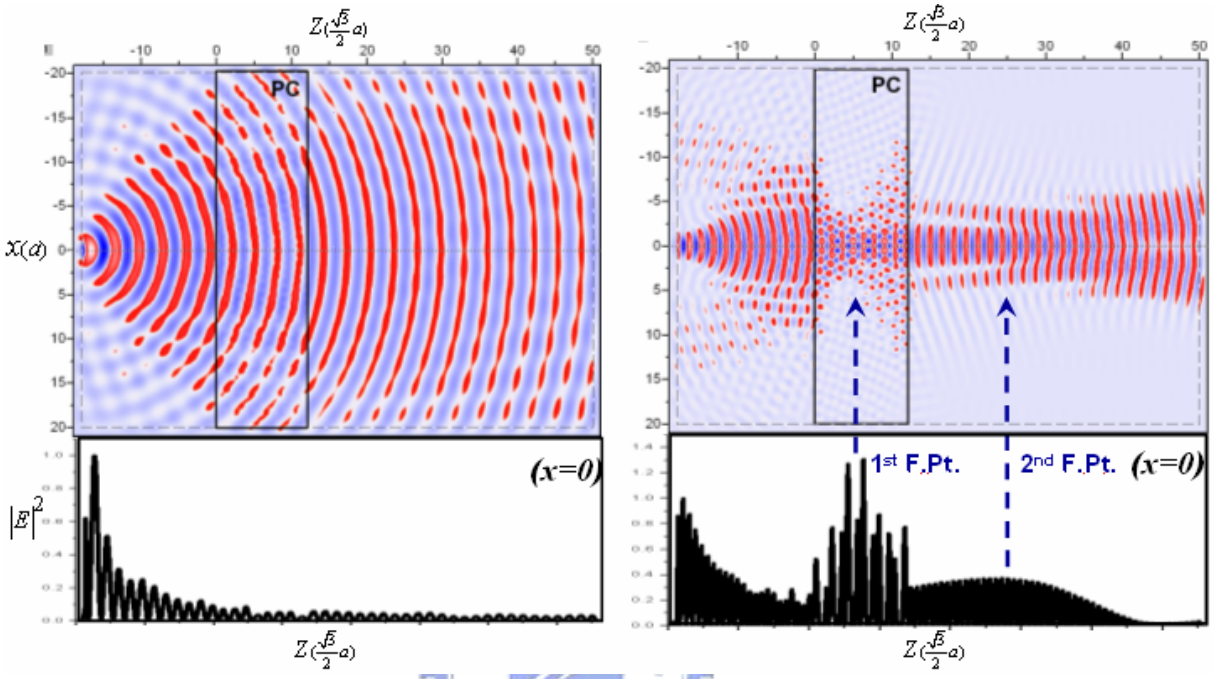

Fig.3-16 FDTD simulations of wave propagation at the frequency of (a) 0.15, and (b) 0.3. Blue, white, and red correspond, respectively, to negative, zero, and positive E_y. (c) and (d) are the plots for longitudinal distribution of the square of electric field along x=0.

Where the circle of solid line is frequency contour 0.3 in photonic crystal and the circle of dot line is frequency contour in dielectric material. The $k_{||}$ conservation condition given by the dashed vertical line in the figures determines the allowed refracted wave vector $\vec{k}_f$. Wave vectors $\vec{k}_i$ of gradual-spreading wave beam hit the 1st interface along direction ΓM with incline angle. The refractive wave vectors $\vec{k}_{f1}$ are anti-parallel with group velocity $\vec{v}_{g1}$, i.e. $\vec{v}_{g2} \bullet \vec{k}_{f1} < 0$, due to the EFS move inwards with increasing frequency (the circle of solid line), then the left-handed (LH) rule will happen. That is the light will be bend to negative

refraction direction. The same $\vec{k}_{f2}$ and $\vec{v}_{g2}$ will refract into negative across the 2nd interface again, ($\vec{k}_{f2}$ is parallel with $\vec{v}_{g2}$ due to the EFS move outwards from the center with increasing frequency). Observably, the energy flows (i.e. $\vec{v}_{g1}$ and $\vec{v}_{g2}$) propagate collectedly toward the focal points from both sides. The theoretical explication consists with the result of our FDTD simulation as Fig. 3-16(b).

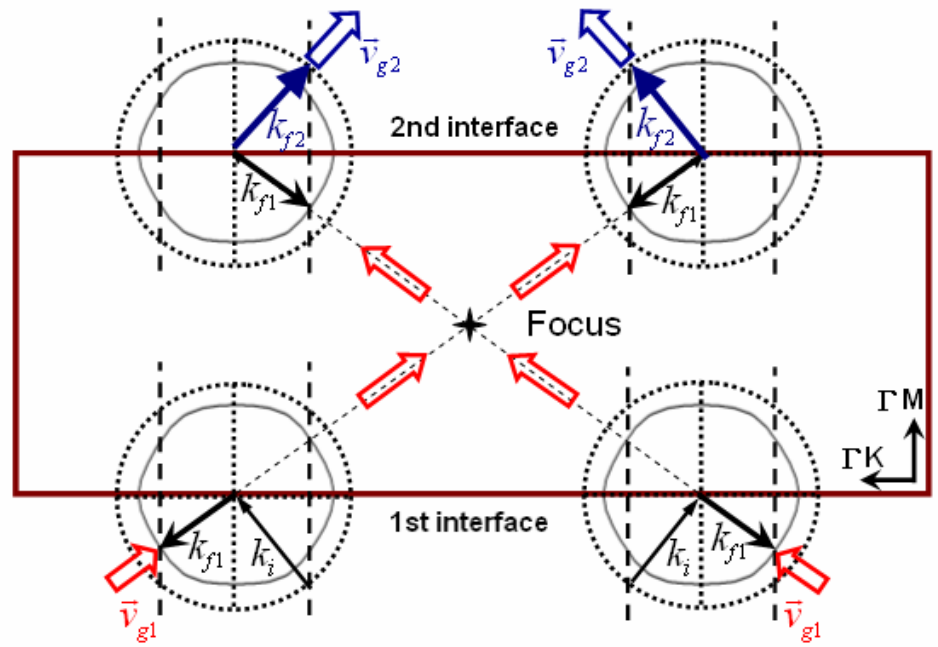

Fig.3-17 Schematic diagram of predicted propagation vectors in real space of the photonic crystal slab with negative refraction behavior. Where the dashed line represents the conservation of the parallel component of the wave vector.

Additional remarks, if we note attentively the Fig. 3-16(d), there is a specific at the 1st first maximum point (i.e. 1st focal point). The 1st maximum value of the square of electric field is larger than the source value! (The all values are normalized with source point=1.) Naturally this doesn't violate the conservation of energy owing to we take only the data along the z axis at x=0. However, the specific implies that light in photonic crystal has a localized effect. It will make electromagnetic field propagate like many wave pockets (particle-like),

and field energy prefer restricting inside the tiny zone.

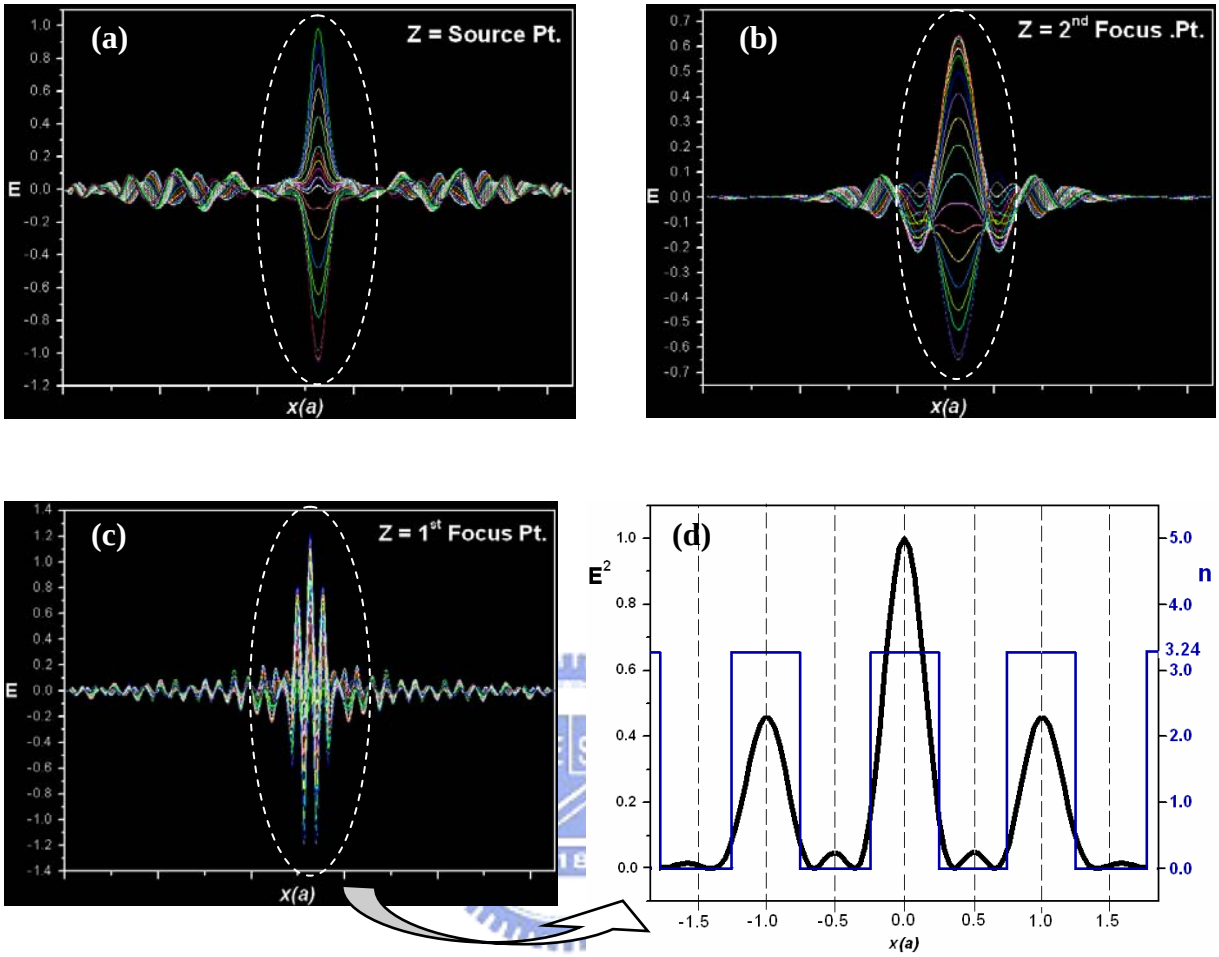

Fig.3-18 Variations of transverse electric amplitude along the x axis are shown as (a) z=source point, (b) z=2nd focal point, and (c) z=1st focal point. (d) Schematics of comparison with the profile of refraction index and square of transverse electric field around the 1st focus.

In Fig. 3-18, the variations of transverse electric amplitude along the x axis are shown as (a) z=source point, (b) z=2nd focal point, and (c) z=1st focal point. (The data are variation with a period of amplitude oscillation.) The wave forms of central part are seen as smooth Gaussian beam due to propagate in isotropic dielectric material, in Fig. 3-18(a) and (b). However, the wave form around the 2nd focus in photonic crystal is divided to few wave pockets which have an extreme sharp form, in Fig. 3-18(c). In addition, we also describe a comparison with the profile of refraction index and square of transverse electric field around

the 1st focus, in Fig. 3-18(d). As the diagrams indicate, the field energy strongly confined in the dielectric region, and the field energy in air region is almost only 5 %, where the index of dielectric is 3.24 (i.e. ε=10.5).

3-3.2 Contrast to imaging in conventional lens and photonic crystal slabs

Pendry predicted firstly that a negative index material (NIM) slab could behave as a ‘‘perfect’’ lens [2], i.e. superlensing effect, which resolution is well below the diffraction limit inherent in conventional lenses. Exhilaratingly, the photonic crystals can perform the negative refraction in the optical regime, moreover, this negative refraction leads to many anomalous light propagation phenomena, e.g., imaging effect.

Fig. 3-19(a) and (b) schematically illustrate two types of imaging individually [9]. We know that imaging by a conventional lens is described by Newton's formula, $(x, y, z) \to (x, y, -\beta z)$ where $\beta = f^2$, in which the focal length is an important parameter. Magnification depends on the relative distance of an object from the lens and focus point. Therefore it only produces a two-dimensional image on the focal plane and does not produce a three-dimensional (3D) image. On the contrary, a negatively refractive photonic crystal produces a 3D image (if it is a three-dimensional negatively refractive photonic crystal) by the mirror-inversion transformation $(x, y, z) \to (x, y, -\beta z)$ where $\beta = abs(n_{eff} / n_0)$, which is different from Newton's formula. The apparent difference between a photonic crystal and a mirror is that the former produces a real image but the latter only produces a virtual image.

Besides, we simulate two cases: the sources (point source) are at 8-times (d_1) and 4-times (d_2) period-z away from the surface of photonic crystal slab, as shown in Fig. 3-20(a) and (b)

respectively. The parameters of photonic crystal structure are same as the former case in section 3-2. As the Fig. 3-12 indicates, the frequency of incident wave is 0.307 when $n_{eff} = -1$.

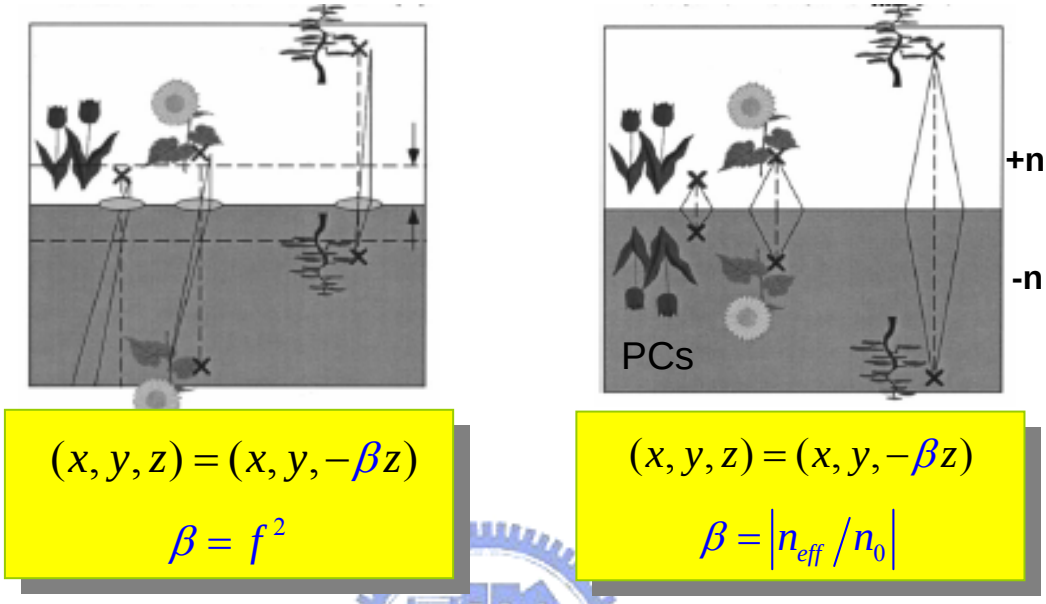

Fig.3-19 Schematics of (a) imaging by a conventional lens, and (b) imaging by a negatively-refractive photonic crystal

For simplifying observation, we adopt this simulative frame what an incident point source produce into photonic crystal slab with $n_{eff} = -1$ from the air with $n = +1$. The imaging effect (i.e. superlensing) can be described similar to the published in Ref.2. Light formerly diverges from the source and refracts through the slab by a negative angle, then converges back to a focal point inside slab; further, generated an image after the light emerging from the slab, as shown in Fig. 3-20(a) and (b). However, the quite large aberrations are visible clearly in the field patterns. We think that a strong-modulated effect caused the aberrations due to the scale of wavelength is similar to the period of photonic crystal, in addition the imaging location still lays in the region of near field.

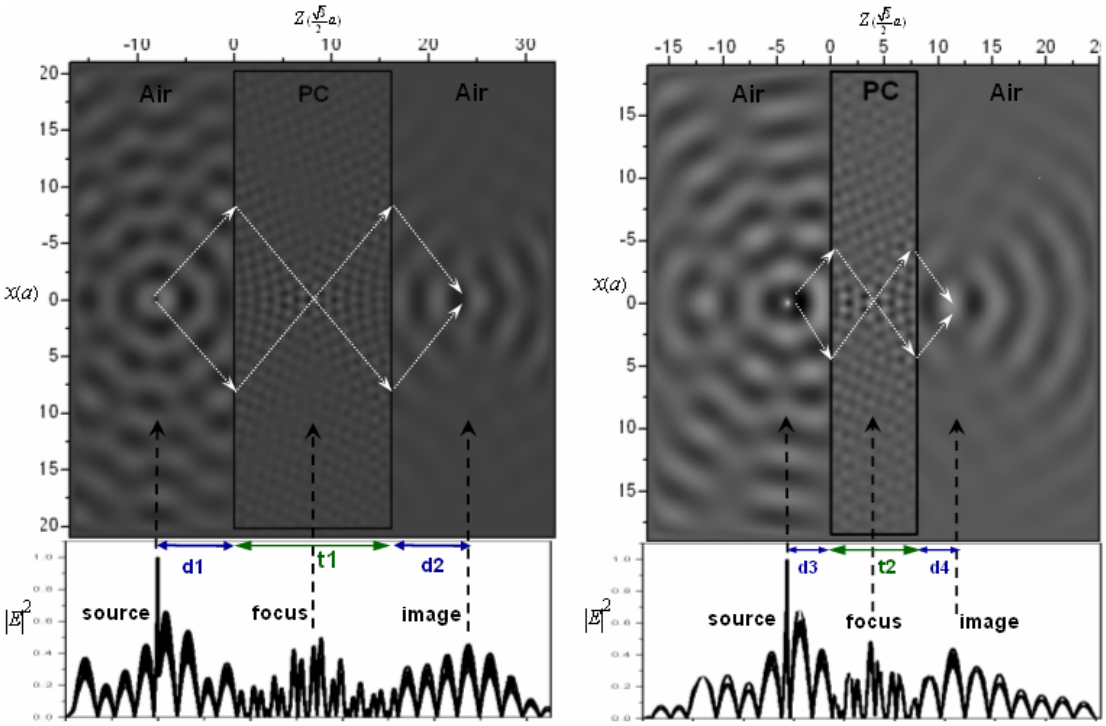

Fig.3-20 The FDTD simulations of imaging by negatively-refractive photonic crystal slabs, frequency of point source is 0.307, place the source at (a) d_1 is 8-times and (b) d_3 is 4-times period-z away from the slab surface respectively. Where the effective refraction index of photonic crystal is -1. The $d_1=d_2$ and $d_3=d_4$.

Results of simulation show that $d_1 \fallingdotseq d_2$ and $d_3 \fallingdotseq d_4$ (i.e. objective distances approximate to imaging distances). Then, according to the result, we can deduce: “that distance of imaging is direct proportional to distance of source, using the center of photonic crystal slab as datum plane”. It’s so strange, because the result is just right opposite to case of conventional lens! As a matter of fact, we know that curvature of lens is employed in focus light, that is, conventional lens use difference of optical path to imaging, as shown in Fig. 3-19(a). For the propagation waves through a flat interface, lens is a non-uniform distribution of refractive index, but photonic crystal slab is a uniform-like distribution by effective refractive index. In other words, if the distance of source becomes longer, then the wave front will become flatter and refractive angle also become smaller. In view of this reason, the imaging position will appear farther from the right-side of slab, as shown in Fig. 3-20(a). Nevertheless, if the

distance of source becomes shorter in Fig. 3-20(b), then result of this case is essential contrary. One can find that the thickness of photonic crystal slab must be double of the objective and imaging distances ($t_1 = 2d_1 = 2d_2$ and $t_2 = 2d_3 = 2d_4$). Therefore, we accordingly understand why imaging via the photonic crystals with negative refractive index is different from the conventional lens.

3-4 Imaging-like phenomena in photonic crystals without negatively effective refraction index

3-4.1 Comment on "All-angle negative refraction without negative effective index" (Phys. Rev. B 65, 201104 (2002))

Lately we paid attention to an interesting opinion that negative refraction in photonic crystals could be realized at fundamental band, i.e. a frequency region without negatively effective refraction index. It's was astonishing and unimaginable to us!

Luo *et al.* proposed that all-angle negative refraction effect does not employ a negatively effective index. [11] Their focus is on the lowest photonic band (fundamental band) near a Brillouin-zone corner farthest from Γ; remarkably, this band has a positive group velocity and a positive effective refraction index, and could be obtain this superlensing [2] presuming through the all-angle negative refraction. Presently we try to recalculate this issue by the same system which is a two-dimensional photonic crystal slab consisting of a square-lattice air-rods in dielectric ε=12.0. The radius of air-rods is 0.35a, where a is the lattice constant. Photonic band structure of TE-mode of this frame in infinite is illustrated in Fig. 3-21(a). Besides, we also have performed finite-difference time-domain (FDTD) simulations on a photonic crystal

slab with parallel side ΓM-direction. In Fig. 3-21(b), descriptively here is a continuous-wave point source of TE-modes with normalized frequency 0.195 placed at a distance 0.35*a* from the left-sided surface. Note the generation of an imaging-like point on the right-sided surface at a distance of 0.38*a*. The obvious result is that the field patterns (H_y field) in the both sides of the slab have a fitting analogue, moreover, wave fronts diverge from the source and image points individually. Our calculated result is in harmony with Ref. 11.

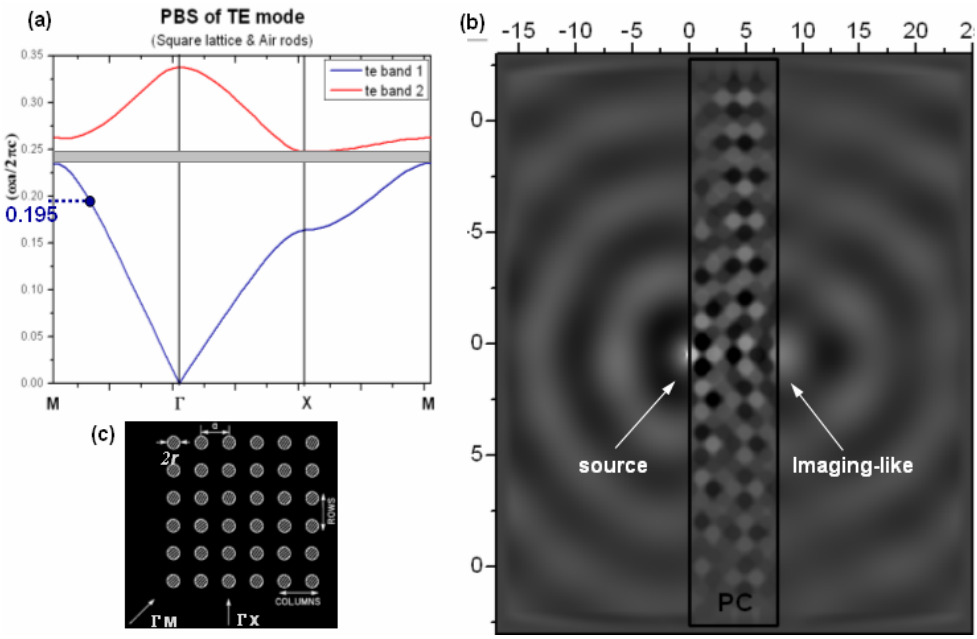

Fig.3-21 (a) TE-mode photonic band structure of 2-D photonic crystal with a square lattice of air rods in dielectric. (b) H_z field of a point source placed at x=-0.35a and an imaging-like across a photonic crystal slab. Dark and bright regions correspond to negative and positive H_z. (c) Square-lattice configuration, showing the lattice a, air-rod radius r, and principal symmetry directions (ΓM and ΓX).

Judging from this viewpoint, we seem to carry out what the photonic crystal slab can do a role-playing as superlens. Nevertheless, this is must be examined attentively. From the previous section, the imaging in photonic crystal slab with a flat surface ought to be observed twice inside and right-sided of the slab following a source diverging. Therefore we will take a process which the point source gradually shifts farther from the photonic crystal slab, and

look what happens to the imaging effect in this system. In Fig. 3-22, the FDTD calculated the wave propagation in photonic crystal slab using a point source located at the left-sided surface with distances of (a) $z=-0.7a$, (b) $z=-2.1a$, and (c) $z=-3.5a$, individually. Where the normalized frequency of source is 0.195 in fundamental band and the thickness of slab is 9-rows.

A distinguishable performance what the wave propagating inside of the slab doesn't feel the negative-refractive modulation due to the periodic structure; the wave fronts appear that aligned proceeding and non-focusing. Besides, the wave beams directly present diverging formation in the left-sided slabs, moreover, analogical circumstances are sighted by us in all the three figures and more obvious following the source departing from the slab. If we take these results to compare with the imaging mechanism by negative refraction (i.e., superlensing effect) in Fig. 3-20, an imaging-like effect of the photonic crystal slab without negatively effective refraction index must be doubted and redefined.

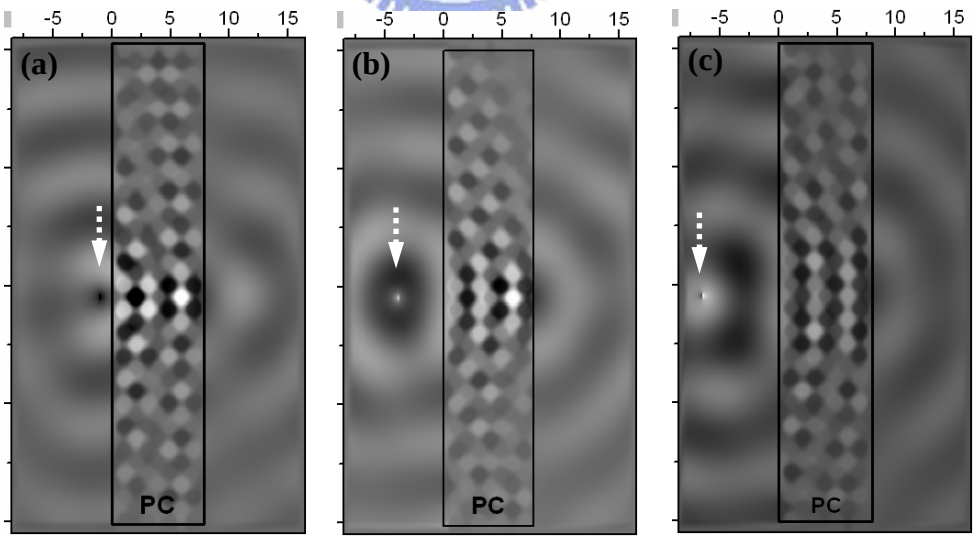

Fig.3-22 FDTD simulations of wave propagation showing the point sources are located at the left-sided PC slabs with a distance (a) 0.7*a*, (b) 2.1*a*, and (c) 3.5*a* from the surface of slabs. These positions with a arrow are the point sources. Where the thickness of PC slabs is 9-rows.

Furthermore, we also tried another simulative case, that is, the number of rows of the PC slabs is changed and the point source still fixed at a distance 0.35*a* from the left-sided surface. The FDTD simulations with PC slab thickness 5-rows, 9-rows, 13-rows, and 17-rows are performed again in Fig. 3-23(c), (a), (d), and (b), respectively. Meanwhile, we discover an inviting result! In cases (a) and (b), the source fields are in phase with the imaging-like fields, in other words, field patterns of the both positions are all positive-orientated H_y synchronously. However, in cases (c) and (d), the source fields are π out of phase with the imaging-like fields, i.e., the imaging-like position and source position have opposite-orientated H_y to each other. Let us associate with a condition of the conventional geometrical optics: image of lens is upright due to a source outside the focal point or is inverted due to a source inside the focal point. Maybe you think that difference in thickness of photonic crystal slab is relative to the imaging behavior with positive or negative quality. In fact, it's only a coincidence! Because the thickness of slabs are just 3-periods and 6-periods of wavelength inside slab, as Fig. 3-23(a) and (b), the emerging light at right-side of slab will be in phase with the source. However the thickness of others is 1.5-periods and 4.5-periods of wavelength inside slab, as Fig. 3-23(c) and (d), so the emerging light will be out of phase with the source.

Lastly we must reiterate an important viewpoint that imaging-like phenomena (i.e., all-angle negative refraction) in photonic crystal slab without negatively effective index exists some serious faults! The phenomena are not certainly real imaging effect in photonic crystals. To realize it, we prefer to define afresh and give the more complete and rigorous conclusions in the following section.

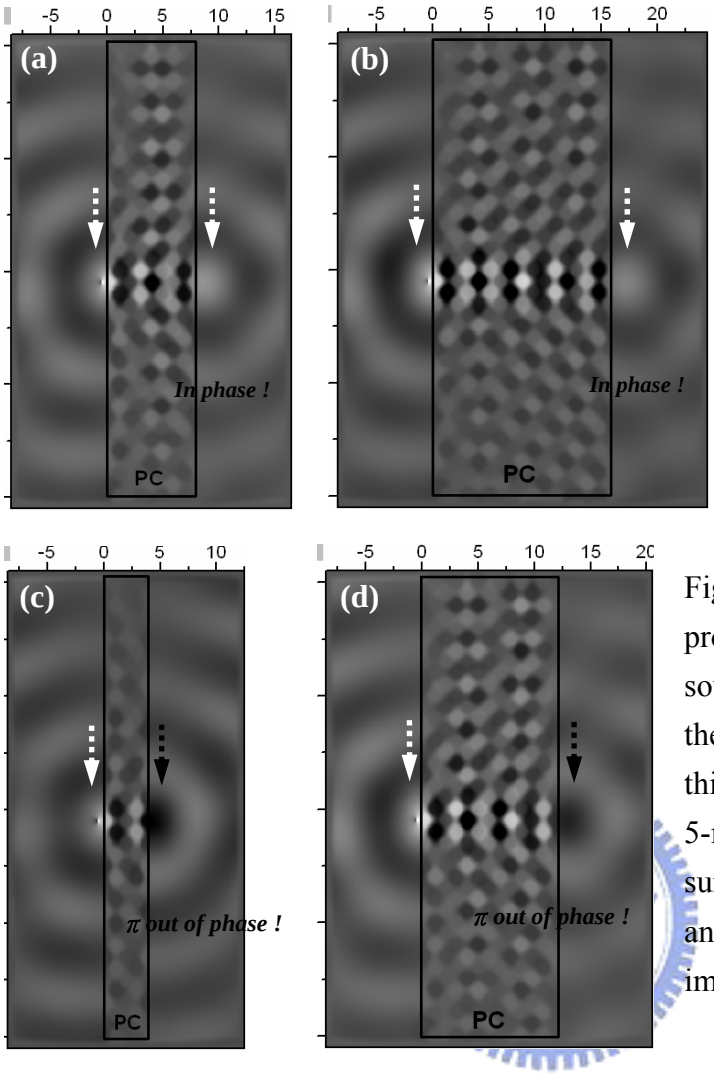

Fig.3-23 FDTD simulations of wave propagation showing the point sources are located at x=-0.35a, and the photonic crystal slabs with a thickness (a) 9-rows, (b) 17-rows, (c) 5-rows, and (d) 13-rows from the surface of slabs. These positions with an arrow are the source points and imaging-like points.

3-4.2 Direct-tunneling effect

As seen in Fig. 3-21(a), a complete TE-mode band gap opens between the first and second bands, and the dashed line stands for the normalized frequency 0.195, in Γ M direction, which lies on the fundamental band with positively effective refraction index, as illustration in section 3-2. Why did a likely negative refraction occur at this region? We will take a dissection about the topics presently.

Schematics of predicted propagation vectors by the equal frequency surface (EFS) can be

analyzed again. Fig. 3-24(a) shows the equal frequency surface (EFS) plot for the fundamental band of a square-lattice photonic crystal with air rods, between the normalized frequencies 0 and 0.24, which is calculated by using plane-wave expansion method. The part of dark-blue shade has a higher frequency and the square area (dash line) is first Brillouin zone. The shape of contours around the central region is almost circular, and the group velocities are parallel with the *k* vectors everywhere. That is indicating the refractive behaviors like isotropic medium at these frequencies, and the concept of effective refraction index can be used for described by the Snell's law. However, the shape of contours turns into flat gradually when moving to the higher frequencies region. We name these contours "flat bands", which lie in the ΓM directions in the figure.

Now we enlarge the part of the first quadrant of Fig. 3-24(a) as shown in Fig. 3-24(b). Where the circle of bold line is frequency contour 0.195 (ω_{PC}), and the circle of dot line is frequency contour in air (ω_{air}). An incident wave vectors $\vec{k}_i$ hits the interface along direction ΓM with incline angle. The $k_{\parallel}$ conservation condition given by the dashed vertical line in the figures determines the allowed refracted wave vector $\vec{k}_f$. As the direction of group velocity $\vec{v}_g = \nabla_k \omega$ is normal to EFS and toward frequency increasing way, the excited Bloch's wave vectors within photonic crystals will point forward owing to a flat band exists on this contour with frequency 0.195. In other words, the refractive waves in photonic crystals propagate directly from the interface.

A mentionable viewpoint, the direct propagations can be achieved at the most parts in this band except at both the bend corners with a larger angle. We can find that a similar negative refraction exhibits at this corner, possibly this is why the all-angle negative

refraction is proposed by using a photonic crystal slab without negatively effective index in Ref.11. In fact, we think a quite serious mistake exists in this argument.

In Fig. 3-25, a FDTD simulation of wave propagation shows the point source is located at x=-0.35a, and the thickness of photonic crystal slab is 25-rows. First the point source is placed extremely near the photonic crystal slab, so the diverging angle of the incident wave will be restrained in a narrow zone. As the prediction in EFS, all of the refractive wave components ought to propagate directly across the slab. The emerging light at right side of the slab diverges again as a point source owing to a very tiny beam width, so it is not an image of the photonic crystal slab!

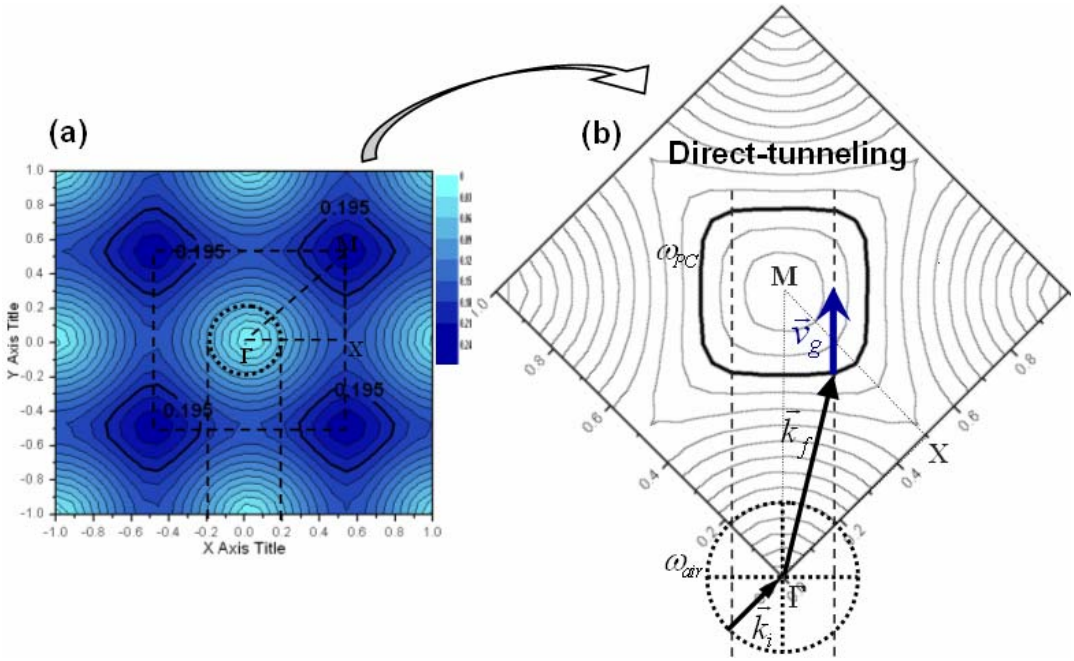

Fig. 3-24 (a) Schematic pictures of the equal frequency surface (EFS) for the 1st band of square-lattice photonic crystal, normalized frequencies 0－0.24, The part of dark-blue shade has a higher frequency. (b) An amplified picture of the part of first quadrant. Where the bold line is for the frequency 0.195 and the dot lines are for the frequency in the air. The dashed line represents the conservation of the parallel component of the wave vector.

Because of more thick slab we can find distinctly that directly propagated waves are confined to the central part of slab (i.e. neighborhood along the x=0). This phenomenon is looked like the photons directly tunneling a narrow channel; we define it as "direct-tunneling effect". The new explanation is we proposed can be consistent with the rule in fundamental band without negatively effective index, furthermore, the direct-tunneling effect also is able performed on the other flat bands of EFS.

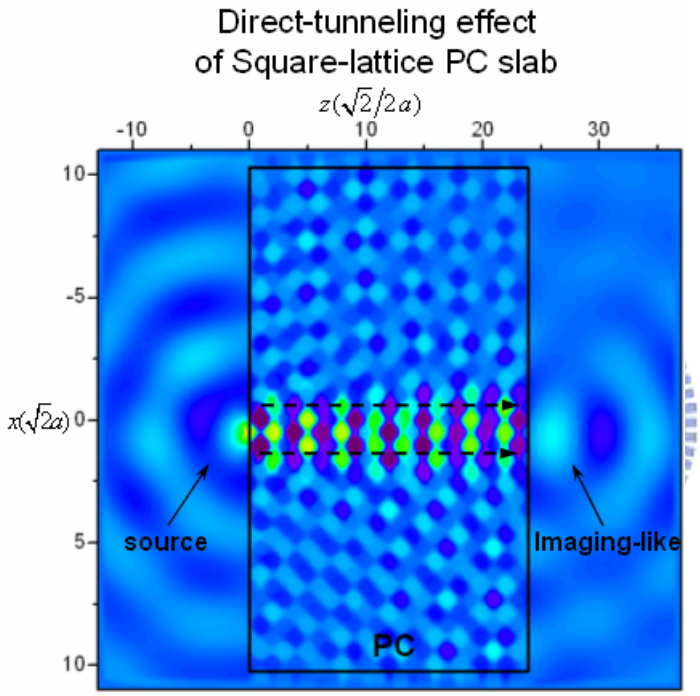

Fig.3-25 FDTD simulation of wave propagation showing a point source is located at x=-0.35a, and the photonic crystal slab with a thickness 25-rows from the surface of slabs.

As well the direct-tunneling effect can be presented by the certain frequencies lie on the flat bands of a triangular-lattice case. We build a simulative frame of triangular-lattice photonic crystal slab with parameters same as the section 3-2. In Fig. 3-26(a), a photonic band structure with the 1st band and 2nd band is shown, and the dashed line indicates the incident normalized frequency 0.2 on the ΓK direction of 1st band. Obviously, the shape of EFS contour for this frequency looks flat around the ΓK direction, as shown in Fig. 3-26(b); so we expect the refractive wave vectors should propagate directly at the flat region of this band.

An imaging-like sight (i.e. all-angle negative refraction) in the triangular-lattice photonic crystal slab without negatively effective index is performed again by utilizing a FDTD calculation in the Fig. 3-26(c). Of course we can conclude that a direct-tunneling effect happens and promotes the imaging-like phenomenon at this time. Apparently the light is strongly confined in a channel-like around the center of slab, moreover, the wave directly tunnels across the slab and diverges again same as a point source after the light emerging from the slab.

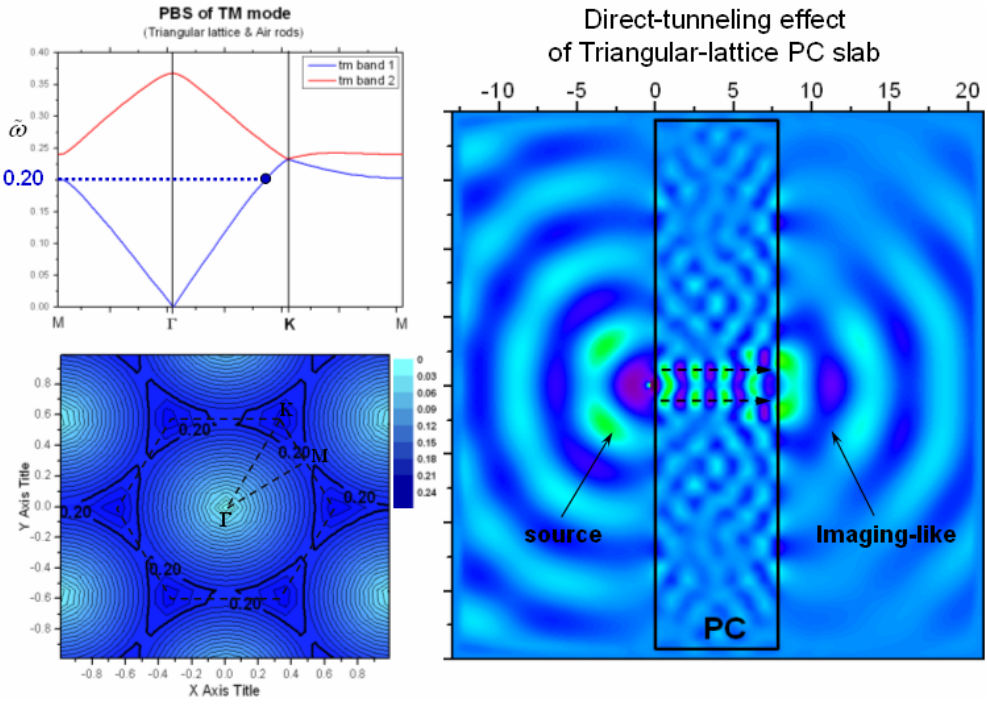

Fig. 3-26 (a) TM-mode photonic band structure of a photonic crystal with triangular-lattice air rods in dielectric. (b) Schematics of the equal frequency surface (EFS) for the 1st band of triangular-lattice photonic crystal, normalized frequencies 0—0.24, The part of dark-blue shade has a higher frequency. (c) E_z field of a point source placed at x=-0.35a and direct-tunneling effect is presented within the photonic crystal slab.

In this section, our analysis of the EFS and FDTD simulations point out that mistaken opinions for the "all-angle negative refraction without negative effective index" and clarify

afresh on this issue utilizing a direct-tunneling effect. In other words, the imaging-like behaviors are not established by a negative refraction law, but preferably by a dominant direct-tunneling effect.